THE JOURNAL OF PHYSICAL CHEMISTRY B

Article

pubs.acs.org/JPCB

Bulk and Single-Molecule Fluorescence Studies of the Saturation of the DNA Double Helix Using YOYO-3 Intercalator Dye

Sergio G. Lopez,[†,§] Maria J. Ruedas-Rama,[†] Salvador Casares,[‡] Jose M. Alvarez-Pez,[†] and Angel Orte*[,†]

[†]Department of Physical Chemistry, Faculty of Pharmacy, University of Granada, Cartuja Campus, 18071, Granada, Spain

[‡]Department of Physical Chemistry, Faculty of Sciences, University of Granada, Fuentenueva Campus, 18071, Granada, Spain

Supporting Information

ABSTRACT: We report a thorough photophysical characterization of the interactions between double-stranded DNA (dsDNA) and the trimethine cyanine homodimer dye YOYO-3. The fluorescence emission of this dye is enhanced by intercalation within the DNA double helix. We have explored the saturation of the dsDNA by bound YOYO-3 at the single-molecule level by studying the single-pair Förster resonance energy transfer (FRET) from an energy donor, Alexa Fluor 488, tagged at the 5′ end of the double helix and the energy acceptor, YOYO-3, bound to the same DNA molecule. The spontaneous binding of YOYO-3 gives rise to an effective distribution of different FRET efficiencies and, therefore, donor−acceptor (D−A) distances. These distributions reveal the existence of multiple states of YOYO-3. Steady-state and time-resolved fluorescence and circular dichroism confirmed the presence of a DNA-bound aggregate of YOYO-3, conspicuous at high dye/base pair ratios. The spectral features of the aggregate suggest that it may have the structure of a parallel H-aggregate.

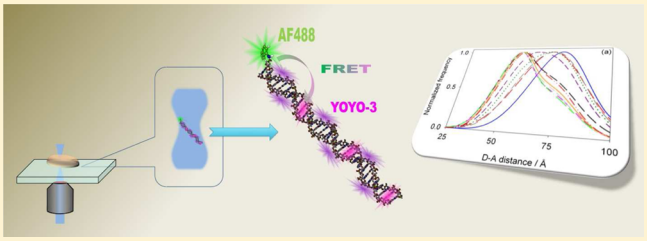

INTRODUCTION

Fluorescence-based biosensor strategies provide high sensitivity because of their ability to offer both high signal and minimal background noise.[1,2] In particular, Förster resonance energy transfer (FRET) has been used to develop analytical methods suitable for the investigation of the extent of selective binding by observing proximity effects causing changes on fluorescence intensity and lifetime.[3,4] In the past few years, the use of small-volume, low-concentration fluorescence measurements in the life sciences has increased dramatically.[5,6] Single-molecule fluorescence spectroscopy, SMFS, offers the ultimate sensitivity because individual molecules can be probed in small volumes and under low-concentration conditions, setting the basis of superresolution imaging techniques.[7] Although fluorescence imaging methodologies are usually based on emission intensity, FRET is a fluorescence-quenching process that can be measured by the fluorescence lifetime of either the donor or acceptor molecules. Therefore, fluorescence lifetime imaging microscopy (FLIM) offers valuable lifetime-based contrast because the lifetimes are independent of the local probe concentration and often depend on the local environment.[8] FLIM allows the mapping of fluorescence lifetimes with (sub)-nanosecond time resolution; therefore, FRET phenomena measured with a FLIM setup can provide temporal and spatial information about dynamics and molecular interactions at both the ensemble and single-molecule levels.[9]

DNA intercalators are a class of fluorescent dyes that exhibit a remarkable increase in fluorescence quantum yield when they associate with double-stranded DNA (dsDNA). This fluorescence can be used as a highly advantageous analytic signal in nucleic acid biosensor design.[10,11] An interesting field of research is the study of dsDNA topology using superresolution fluorescence techniques. Superresolution fluorescence, such as photoactivated localization microscopy (PALM)[12] or stochastic optical reconstruction microscopy (STORM),[13,14] uses photoswitchable dyes to localize single dyes in real time and reconstruct images with nanometer resolution. Intercalating dyes have been shown to successfully allow for superresolution imaging of dsDNA.[15] Ten years ago, we reported the first instance of FRET between an intercalator and extrinsic fluorophore-labeled DNA to develop a general approach to detect nucleic acid sequences in homogeneous media, combining the use of a fluorescein-labeled single-stranded DNA model probe, a cDNA target strand, and ethidium bromide (EB) as the DNA intercalator.[16] Subsequently, other approaches have used fluorescein attached at a DNA terminus to amplify EB emission signals.[17,18] Nevertheless, all of these approaches suffer from the same drawback, EB intercalators' low dsDNA affinity constants.[19] Dimeric cyanine dyes are a family of fluorophores used in nucleic acid staining because of their intercalating properties. Among the more popular cyanine dyes are the oxazole yellow (YO) homodimers YOYO-1 (1,1′-(4,4,8,8-tetramethyl-4,8-diazaundecamethylene)-bis-4-[3-methyl-benzo-1oxazol-2-yl methylidene]-1,4-dihydroquinolinium tetraiodide) and YOYO-3, a benzoxazolium-4-quinolinium dimer with three carbon atoms bridging the aromatic rings of

Received: April 10, 2012
Revised: September 3, 2012
Published: September 4, 2012

ACS Publications © 2012 American Chemical Society

the unsymmetrical cyanines.[20,21] Both dyes show a fluorescence enhancement factor of approximately 3200 when bound to dsDNA.[21] In addition, their molar extinction coefficients are high (>84 000 M^{-1} cm^{-1}).[21] Moreover, YOYO-1 and YOYO-3 have a greater affinity for DNA than do EB and other cyanine dyes.[22] The strong binding of YOYO, together with its large increase in fluorescence quantum yield upon binding to DNA, have made YOYO very useful for the detection[20,23,24] and fluorescence microscopy imaging of DNA.[25,26]

Studies of its interaction with DNA have shown that YOYO-1 exhibits two different binding modes.[27,28] Its predominant mode of binding is bis-intercalation for dye/DNA base mixing ratios of up to 0.125, with the long axis of the YO chromophore oriented parallel to the long axis of the basepair pocket. For dye/basepair ratios higher than 0.125, a secondary DNA binding mode begins to contribute noticeably.[27] Nevertheless, although these conclusions were well supported, no binding constant values were recovered. The base content and sequence also have different effects on the conformation of the helical structure, creating different chemical environments on the minor and major grooves[29−31] that may affect the binding behavior of intercalative dyes. In one of the most extensive studies on the base-content dependence of emission enhancements, quantum yields, and lifetimes for 10 monomeric and bichromophoric cyanine dyes, Netzel et al.[32] showed that the excited-state decay times of cyanine dyes are multiexponential and dependent on the composition of the dsDNA. Recent single-molecule fluorescence studies using average decay-time distributions have shown that thiazole yellow homodimer, TOTO (another popular cyanine dye),[22,33] intercalated into poly dAdT dsDNA has an average fluorescence lifetime of 1.8 ns, whereas TOTO intercalated into poly dGdC dsDNA has an average fluorescence lifetime of 2.2 ns.[34] This small lifetime difference has been used at the single-molecule level to estimate the GC content of oligonucleotides with intermediate GC compositions to within a few percent error and to determine the relative binding affinity of TOTO for different dsDNA fragments.[34]

In recent papers, we reported an investigation on the photophysics and binding properties of the homodimeric cyanine dye BOBO-3 with DNA oligonucleotides.[35−37] Using time-resolved fluorescence, we showed that BOBO-3 interacts with dsDNA according to two different binding modes, a low-affinity mode and the clamp-like bis-intercalation mechanism. The quantification of the contributions in each binding mode showed that the dye is distributed according to similar affinity constants: $(8.8 \pm 1.1) \times 10^5$ M^{-1} for the intercalating mechanism (covering 5.9 ± 0.2 sites) and $(2.6 \pm 0.3) \times 10^5$ M^{-1} (covering 3.5 ± 0.5 sites) for the low-affinity mode.[27] Nevertheless, these recovered affinity constants are too small for the study of the photophysics and intercalation properties of cyanine intercalators by SMFS due to the low concentrations needed for the single-molecule regime. Therefore, the use of intercalator dyes in SMFS requires larger affinity constants to prevent the dye from dissociating from the oligonucleotide when diluted to the single-molecule level.[34] Because of both the high affinity constant and the large fluorescence enhancement described for YOYO when bound to dsDNA, we have chosen YOYO-3 as a suitable dye for SMFS studies. In addition, its spectral properties make YOYO-3 a good acceptor for FRET studies when the energy donor is a rhodamine-based dye, such as Alexa Fluor 488 (AF488), labeling an oligonucleotide strand.

In this paper, we present a thorough study of the behavior of YOYO-3 with dsDNA under ensemble conditions and the energy transfer from a donor dye AF488 labeling the dsDNA toward the intercalator YOYO-3 under single-molecule conditions. Our interest here lies in characterizing the energy transfer, physical behavior, and interactions between the dye species involved in the FRET-based transduction strategies we propose. This study provides the basis for the development of an intercalator-based FRET strategy for signaling nucleic acid hybridization events at the single-molecule level, the first step in developing a methodology ultimately intended for use in a nucleic acid biosensor.

EXPERIMENTAL METHODS

Chemicals and Sample Preparation. YOYO-3 iodide (Scheme 1) stock solution was purchased from Invitrogen

Scheme 1. Molecular Structure of YOYO-3

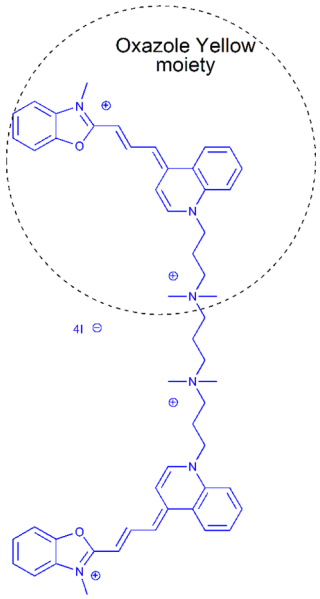

(USA). The chemically synthesized oligonucleotide sequence (5′-ATG CTA GGC AGG TAA CTA CTC GAT AAG CGA TAC AGA ATG GCA GTA-3′) and its complementary strand were obtained from IBA Technologies (Germany). For single-molecule FRET, the same oligonucleotide sequence was labeled at the 5′ end with an AF488 dye molecule (IBA). All oligonucleotide strands were purified by double HPLC. The single-stranded DNA sequences were annealed with their corresponding complementary strand to form the respective double-stranded DNA (dsDNA). The hybridization was performed by heating at 95 °C for 5 min and slowly cooling to room temperature. Stock solutions of YOYO-3 and 45 basepair (bp) oligonucleotides were prepared separately using TEN buffer (10 mM Tris, 1 mM EDTA, and 100 mM NaCl) (Sigma-Aldrich, Spain) as the solvent. Dye and DNA concentrations were determined spectrophotometrically using $\varepsilon_{(611\ nm)} = 9.42 \times 10^4$ M^{-1} cm^{-1} for YOYO-3 and $\varepsilon_{(260\ nm)} = 4.70 \times 10^5$ and $\varepsilon_{(260\ nm)} = 4.13 \times 10^5$ M^{-1} cm^{-1} for the tagged oligonucleotide sequence and its complementary strand, respectively. In intercalation experiments, YOYO-3 was mixed with the dsDNA solutions in different proportions to obtain a wide range of dye-to-bp ratios (d/bp) and incubated for 10 min in the dark at 25 °C. All chemicals were used as received. Prior

dx.doi.org/10.1021/jp303438d | J. Phys. Chem. B 2012, 116, 11561−11569

to each measurement, samples were stirred for at least 3 min at 25 °C.

Time-Resolved Fluorescence and Fluorescence Anisotropy Measurements. Fluorescence lifetime and anisotropy decay measurements were recorded in time-correlated single-photon counting (TCSPC) mode using a FluoTime 200 fluorometer furnished with a TimeHarp 200 collection card and equipped with a fiber-coupled 531 nm LDH-P-FA-530 pulsed laser working at a 20 MHz repetition rate (PicoQuant GmbH, Germany). The instrument response function (IRF), measured using a Ludox suspension, has a full width at half-maximum of ≈330 ps. All decays were recorded until reaching 2×10^4 counts in the peak channel. For those samples used for emission measurements, the peak absorbances were kept lower than 0.08 to avoid fluorescence reabsorption. However, because of its low fluorescence quantum yield, Φ_f, higher peak absorbances ($A = 0.19$) were required to obtain the emission and excitation spectra of YOYO-3. All measurements were performed at room temperature (ca. 25 °C) using 4 × 10 mm quartz cuvettes.

Fluorescence decay traces were deconvoluted with the IRF and fitted, using the FluoFit 4.4 package (Picoquant GmbH), to multiexponential functions via a Levenberg−Marquard nonlinear least-squares minimization algorithm. Unless otherwise specified, three different exponential terms were used to fit the experimental decay traces of YOYO-3 in the presence of dsDNA. The quality of the fits was determined by the reduced chi-squared method, χ^2, the weighted residuals, and the correlation functions. The latter two were checked for random distributions. To estimate the energy transfer efficiency, the amplitude-averaged decay times were determined using eq 1[38]

$$<\tau_f> = \frac{\sum_{i=1}^{n} \alpha_i \tau_i}{\sum_{i=1}^{n} \alpha_i} \quad (1)$$

where α_i are the pre-exponential factors and τ_i the lifetimes obtained in the multiexponential fitting of the decay traces.

Single-Molecule Measurements. Measurements were performed on a MicroTime 200 fluorescence lifetime microscope system (PicoQuant GmbH, Germany) using the time-tagged time-resolved (TTTR) methodology.[39,40] The TTTR method allows for the reconstruction of the entire fluorescence decay trace from the fluorescence fluctuation trace and performs burst-integrated fluorescence lifetime (BIFL) analysis.[41,42] BIFL analysis estimates the lifetimes associated with each single-molecule burst selected by applying an adequate threshold. The data analysis was performed using SymphoTime software (PicoQuant GmbH). A 470 nm LDH-P-C-470 pulsed laser (PicoQuant GMbH), working at a 20 MHz repetition rate, was used as the excitation source. The excitation beam was directed onto a dichroic mirror (510 DCXR) and focused on the oil immersion objective (1.4 NA, 100 ×). The sample consisted of a small volume (≈ 80 μL) of solution placed on a clean glass coverslip, which was mounted on the microscope stage. Fluorescence emitted from the sample was filtered by an HQ500LP long-pass filter, passed through a 75 μm pinhole, and separated into two different detection channels by a 600 DCXR dichroic mirror. A bandpass filter was placed in each channel immediately ahead of the detector: a 520/35 bandpass filter in the donor channel (AF488 dye) and a FB650-40 bandpass filter in the acceptor channel (YOYO-3 fluorescence). The fluorescence photons were finally focused onto two SPCM-AQR SPAD detectors (PerkinElmer, USA). A small amount of Tween 20 (≈ 0.001%) was added to the samples to prevent the surface adhesion of the DNA molecules.

The FRET efficiency distributions at the single-molecule level between AF488 and YOYO-3 were explored by selecting fluorescence bursts that surpassed the threshold value of 6 (SUM criterion).[43] We calculated the apparent FRET efficiency, the so-called Proximity Ratio (PR), to construct FRET efficiency distributions for each fluorescence burst using eq 2

$$\mathrm{PR} = \frac{I_{\mathrm{Acc}}}{I_{\mathrm{Acc}} + I_{\mathrm{Don}}} \quad (2)$$

where I_{Acc} and I_{Don} are the background and cross-talk-corrected burst intensities in the acceptor and the donor channel, respectively. The cross-talk from the donor channel into the acceptor channel was 0.049, whereas the cross-talk from the acceptor channel into the donor channel was negligible.

The apparent FRET efficiency, E_{app}, may also be obtained from the donor fluorescence lifetime, τ_{FRET}, using the following equation

$$E_{\mathrm{app}} = 1 - \frac{\tau_{\mathrm{FRET}}}{\tau^0} \quad (3)$$

where τ^0 is the fluorescence lifetime of the unquenched donor; i.e., 4.1 ns for AF488.[22]

The PR and E_{app} distributions were transformed into donor-to-acceptor distance, r, distributions as follows[44]

$$r = R_0\left(\frac{1}{E} - 1\right)^{1/6} \quad (4)$$

where E represents the FRET efficiency in terms of PR or E_{app} and R_0 is the Förster radius.

RESULTS AND DISCUSSION

YOYO-3 Intercalated into AF488-Tagged dsDNA Molecules at the Single-Molecule Level. The high affinity of cyanine dyes toward dsDNA makes these dyes interesting components in the development of ultrasensitive, fluorescence-based DNA sensors. Single-molecule fluorescence techniques offer the ultimate sensitivity because fluorescence emission from individual molecules can be detected, which is extremely useful for studying biological interactions.[45−47] To test the behavior of YOYO-3 down to the single-molecule regime, we performed single-molecule FRET measurements using dsDNA labeled with a donor fluorophore, Alexa Fluor 488 (AF488), at one end and increasing amounts of YOYO-3. We probed the energy transfer between the excited donor toward the acceptor YOYO-3. The combined absorption and emission spectra for DNA-bound YOYO-3 and the oligo-conjugated AF488 in Figure S-1 (Supporting Information) show significant overlap of the AF488 emission spectrum with the DNA-bound YOYO-3 absorption spectrum, indicating that efficient energy transfer may be possible at relatively close distances. The fluorescence quantum yields, Φ_f, of AF488 and DNA-bound YOYO-3 are 0.92 and 0.15, respectively, although YOYO-3 has a negligible quantum yield when free in aqueous solution ($\Phi_f \leq 0.01$).[22] Assuming the complete orientation averaging of the dye transition dipoles ($\kappa^2 = 2/3$), the Förster radius, R_0, for the energy transfer from AF488 to DNA-bound YOYO-3 is 56 Å. However, this R_0 value is not strictly valid for the present system, in which the dynamic averaging regime is not attained due to the limited orientational mobility of DNA-bound

dx.doi.org/10.1021/jp303438d | J. Phys. Chem. B 2012, 116, 11561−11569

YOYO-3. The validity of assuming a value of 2/3 for κ^2 will be discussed later. The dsDNA molecules used in this work are expected to be rigid due to their short length (45 bp); therefore, the bending of these dsDNA molecules should have a negligible influence on the donor−acceptor distance.[48]

We collected fluorescence burst traces at the single-molecule level using 200 pM of labeled dsDNA and increasing concentrations of YOYO-3 in the 75−1000 nM range. Although the concentration of YOYO-3 is larger than that required for SMFS measurements, the equilibrium between intercalated YOYO-3 and free YOYO-3 is shifted toward the dissociated species at such low concentrations. Therefore, the equilibrium must be pushed toward the formation of the intercalated YOYO-3 by increasing its concentration. The very low fluorescence emission of free YOYO-3 in solution just causes a slight increase in the background fluorescence. This background can easily be removed by applying appropriate threshold values in the burst-picking analysis. In our experiments, we employed a pulsed laser to excite molecules and instrumentation with time-resolved fluorescence capabilities, facilitated by the TTTR collection methodology.[39,40] This approach allows us to not only collect single-molecule fluorescence bursts but also explore single-molecule fluorescence lifetime distributions (FLDs) and reconstruct the fluorescence decay traces.

The overall AF488 fluorescence decay histograms, constructed by combining the individual contributions of all of the measured single molecules, can be found in Figure 1a. It is evident from this figure that the AF488 fluorescence lifetime shortens with increasing YOYO-3 concentration. The FLDs from the donor dye, AF488, were obtained by assigning a single average lifetime to each detected fluorescence burst from individual molecules and using the maximum likelihood estimator and BIFL analysis. As shown in Figure 1b, the FLDs shift to shorter times with increasing YOYO-3 concentration, as expected for a nonradiative energy transfer mechanism. Moreover, the distributions narrow at high YOYO-3 concentrations, suggesting that energy transfer occurs preferentially toward those YOYO-3 molecules located closer to the AF488 dyes in highly loaded DNA strands.

We also studied the FRET efficiency in these samples by analyzing the fluorescence bursts in both the donor and the acceptor channel. In the AF488 detection channel, the number of fluorescence bursts per second decreases with increasing YOYO-3 concentration (Figure 2a), whereas an increase in the burst rate is observed up to 0.3 μM YOYO-3 in the YOYO-3 detection channel, followed by a decrease at higher YOYO-3 concentrations (Figure 2b). The increase in the number of bursts per second observed at low YOYO-3 concentrations, combined with the concomitant quenching of AF488 fluorescence, is strong evidence of resonance energy transfer from AF488 to YOYO-3. Nevertheless, instead of a continuous increase in the acceptor burst rate, a further decrease in YOYO-3 fluorescence bursts at higher concentrations was observed. This decrease suggests an additional quenching of the acceptor dye that must be caused by an increase in the nonradiative deactivation rate,[49,50] or energy hopping.[51,52] This observation

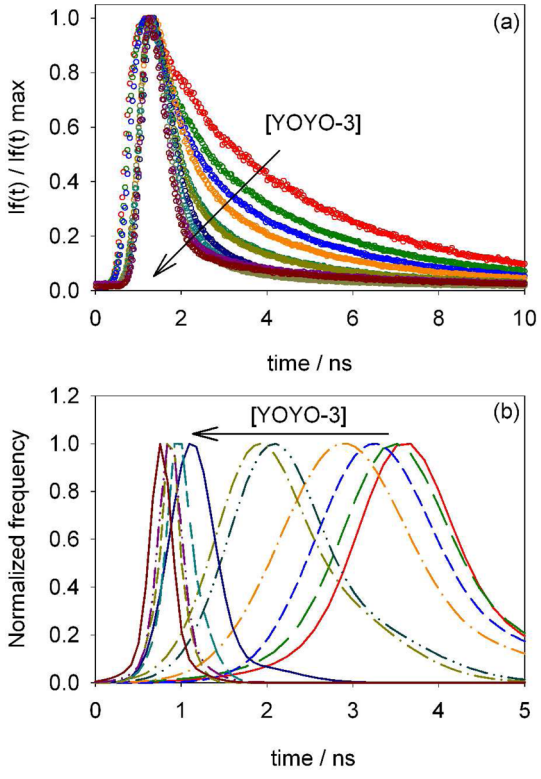

Figure 1. (a) AF488 fluorescence decay histograms from single-molecule fluorescence traces of samples containing 200 pM AF488-dsDNA (45bp) and 0.000, 0.075, 0.100, 0.200, 0.300, 0.375, 0.438, 0.500, 0.625, 0.675, and 1.000 μM YOYO-3. λ_{ex} = 470 nm. (b) The corresponding fluorescence lifetime distributions of single-molecule fluorescence bursts, analyzed by BIFL.

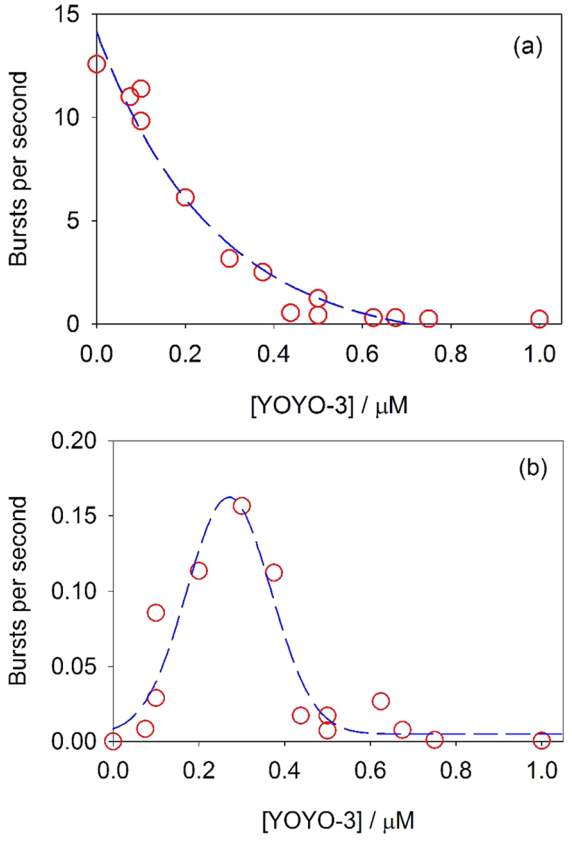

Figure 2. Single-molecule fluorescence burst rates registered on the AF488 (a) and YOYO-3 (b) detection channels from solutions containing 200 pM of labeled dsDNA and increasing concentrations of YOYO-3. Dashed lines are introduced for illustrative purposes only.

dx.doi.org/10.1021/jp303438d | J. Phys. Chem. B 2012, 116, 11561−11569

supports the notion that energy transfer occurs from FRET-excited acceptors toward other intercalated units, in an antenna-like process.[53]

Donor−acceptor (D−A) distance distributions from burst picking were calculated according to eqs 2 and 4. The distance separating the donor from the acceptor can be estimated from the FRET efficiency values provided that the orientation factor, κ^2, is known. If the transition dipoles of the donor and the acceptor sample all orientations (isotropic condition) during the excited-state lifetime of the donor (dynamic averaging condition), the average orientation factor $\langle\kappa^2\rangle$ is 2/3 (isotropic dynamic averaging condition). If the isotropic condition is not fulfilled but the dynamic averaging condition is, a single value for $\langle\kappa^2\rangle$ cannot be provided; therefore, it is necessary to gauge the lower and upper boundaries of $\langle\kappa^2\rangle$, which are obtained by measuring the anisotropy decays of the donor and the acceptor. On the contrary, if the dynamic averaging condition is not fulfilled but the isotropic condition is, $\langle\kappa^2\rangle$ cannot be appropriately obtained, although an unsuitable value of 0.476 has been extensively utilized for this particular case.[54] Time-resolved anisotropy measurements and limiting anisotropy values revealed a complex situation in which the existence of energy hopping between molecules of YOYO-3 and YOYO-3 aggregates causes anomalous anisotropy tendencies (see Figure S-3 and details in the Supporting Information), as it has been described for other monomeric and dimeric YO derivatives.[51,52] Therefore, the depolarization factor of the acceptor, required to calculate the lower and upper boundaries for κ^2, cannot be obtained in our case. However, the rotational mobility of AF488, tagging the end of the DNA double helix, is not expected to be hampered in any way; hence, we can assume that the relative orientation of the donor fluorophore with respect to the acceptor YOYO-3 is effectively random. According to Dale et al., for our particular scenario, it is perfectly acceptable to use a $\langle\kappa^2\rangle$ value of 2/3 because the lower and upper boundaries for $\langle\kappa^2\rangle$ are 1/3 and 4/3, respectively, under these conditions.[54] Therefore, the maximum error in the calculation of the donor-to-acceptor distance due to the assumption of 2/3 for $\langle\kappa^2\rangle$ is only approximately 12%. Thus, we transformed the PR values into absolute distances using eq 4 and an R_0 value of 56 Å, obtained by assuming a $\langle\kappa^2\rangle$ of 2/3. Figure 3a shows that, at low acceptor concentrations, the broad distributions peaked around 75 Å, a distance corresponding to 22 basepairs, roughly half the length of the dsDNA chain. Moreover, a shift to shorter D−A distances is observed with increasing YOYO-3 concentration, but this tendency disappears at higher YOYO-3 concentrations, at which the D−A distance reaches a plateau. The onset of this plateau can be appreciated with further clarity by calculating the weighted averages of the D−A distance distributions (Figure 3b). The plateau becomes noticeable at approximately 0.45 μM YOYO-3. Its appearance may be ascribed to the full saturation of the binding sites for YOYO-3 within the dsDNA and to an increase in the nonradiative deactivation rate of YOYO-3, which, in turn, would decrease the value of the proximity ratio. This behavior is, qualitatively, in good agreement with the donor FLDs shown in Figure 1b. Nevertheless, when the donor FLDs were converted into donor−acceptor distances by using eqs 3 and 4 these estimated distances were clearly shorter than those estimated through the PR distributions (Figure 3b). This discrepancy is another evidence of the additional energy hopping decreasing the FRET-excited acceptor sensitized emission. Interestingly, regardless of the methodology

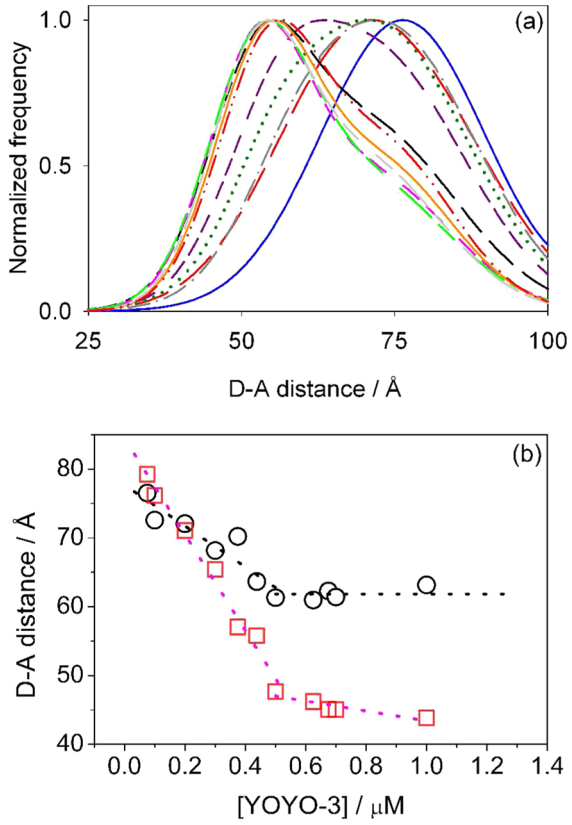

Figure 3. (a) Donor−acceptor distance distributions from single-molecule fluorescence bursts of 200 pM labeled dsDNA and 0.0−1.0 μM YOYO-3. (b) Weighted means of the D−A distance distributions from PR distributions in (a) (circles) and from AF488 FLDs in Figure 1b (squares). The dotted straight lines are introduced for illustrative purposes only.

employed, the donor−acceptor distance plot undergoes a drastic change in the slope at the same YOYO-3 concentration. This concentration indicates the saturation point of the dsDNA with intercalated YOYO-3. When comparing the estimated distances with structural considerations, at high YOYO-3 loadings the distance between the AF488 and the closest intercalated YOYO-3 moiety should not be larger than 40 Å (accounting for the AF488 linker length), and hence FRET efficiencies close to 0.9 would be expected. These structural concerns are in good agreement with the results of donor−acceptor distances obtained via the donor fluorescence lifetime. The energy hopping within the acceptor moieties decreases the apparent FRET efficiency detected by the burst picking method. This additional phenomenon reduces the acceptor-sensitized emission causing an apparent decrease in the estimated FRET efficiency. This clearly demonstrates the superior performance of single-molecule fluorescence with time-resolved capabilities for FRET measurements because the effect over the donor fluorescence lifetime, in this case, is solely caused by FRET and no other effect.

The effect of energy hopping as an additional photophysical process in the FRET between the extrinsic AF488 and the intercalated YOYO-3 molecules has been revealed by the differences found between lifetime-based estimations and burstwise analysis of the FRET efficiency. However, the nature of the species causing the energy hopping remains to be elucidated at this point and will be further investigated in the following section.

dx.doi.org/10.1021/jp303438d | J. Phys. Chem. B 2012, 116, 11561−11569

dsDNA-Bound YOYO-3 Intramolecular H-Aggregate as the Energy Hopping Acceptor. To gain more insight into the nature of the species causing the energy hopping between intercalated YOYO-3 molecules, we performed absorption, steady-state and time-resolved fluorescence, and circular dichroism (CD) experiments in the ensemble regime. The fluorescence intensity of free YOYO-3 in aqueous solution is weak due to intramolecular deactivation[28] and the formation of intramolecular H-aggregates in solution.[55] The hindrance of these two effects upon binding to dsDNA is the main reason underneath the remarkable enhancement in its fluorescence emission. This is evident when comparing the absorption and excitation spectra of YOYO-3 in the absence and the presence of dsDNA (Figure S-2, Supporting Information). The main findings from the absorption and emission spectra of dsDNA-bound YOYO-3 can be summarized as follows (see Supporting Information for details): (1) the shape of the absorption spectrum remains unaltered up to a [YOYO-3]/[DNA bp] ratio of 0.087, (2) the shape of the excitation spectrum is emission-wavelength independent and the shape of the emission spectrum is excitation-wavelength independent, and (3) the shape of the excitation spectrum coincides reasonably well with the shape of the absorption spectrum. The formation of an intramolecular aggregate is supported by the shape of the excitation spectra of free YOYO-3 (Figure S-2, Supporting Information), which is similar to the excitation spectra of intercalated YOYO-3, suggesting that the faint emission observed for free YOYO-3 arises from a small fraction of molecules that do not form the intramolecular aggregate.

Time-resolved fluorescence spectroscopy is an invaluable tool to reveal the kinetics of the photophysical processes taking place in the system, so we carried out measurements to further explore the temporal behavior of YOYO-3 emission. In the presence of dsDNA, the fluorescence decay traces of aqueous solutions containing 0.10−0.80 μM YOYO-3 and 0.01−1.00 μM dsDNA were recorded at 530 nm for excitation and 630 nm for emission. In all cases, the best fits required a sum of three exponential decay functions to reach low χ^2 values in addition to a random distribution of the weighted residuals and autocorrelation function, indicators of the goodness of the fits. Figure 4 shows the fluorescence decay times and their corresponding amplitudes. The decay times and the amplitudes were constant at low [YOYO-3]/[DNA bp] ratios (in the range 0.002−0.089), with values of 3.15 (±0.12), 1.47 (±0.11), and 0.37 (±0.04) ns for the three decay times and 0.28 (±0.02), 0.37 (±0.01), and 0.35 (±0.02) for the respective normalized amplitudes. Considering the absorption, excitation, and emission spectra features, along with the fact that the decay time and amplitude values remain constant through a wide range of low [YOYO-3]/[DNA bp] ratios, it is unlikely that the multiexponential nature of the decay could arise from the coexistence of discrete, different binding modes at these low [YOYO-3]/[DNA bp] ratios. Hence, the multiplicity of the decay times most likely originates from a bulk of dissimilar interaction modes between the excited YOYO-3 molecules and the DNA or different environments on the several sequence sections over the dsDNA. To corroborate such a hypothesis we studied the emission spectra associated to the three decay time components (3.15, 1.47, and 0.37 ns). These species-associated emission spectra completely overlap, suggesting that the three components come from the same species (see Supporting Information, and Figure S-4 for details). The time evolution of the emission spectra in the nanosecond time scale, via the so-called time-resolved area-normalized emission spectra, also confirmed this scenario. These results showed no variation in the emission spectra at 0, 1, and 15 ns after excitation (Figure S-4, Supporting Information), reasserting that the multi-exponential nature of the YOYO-3 fluorescence decay may arise from a bulk of different environments within the dsDNA.

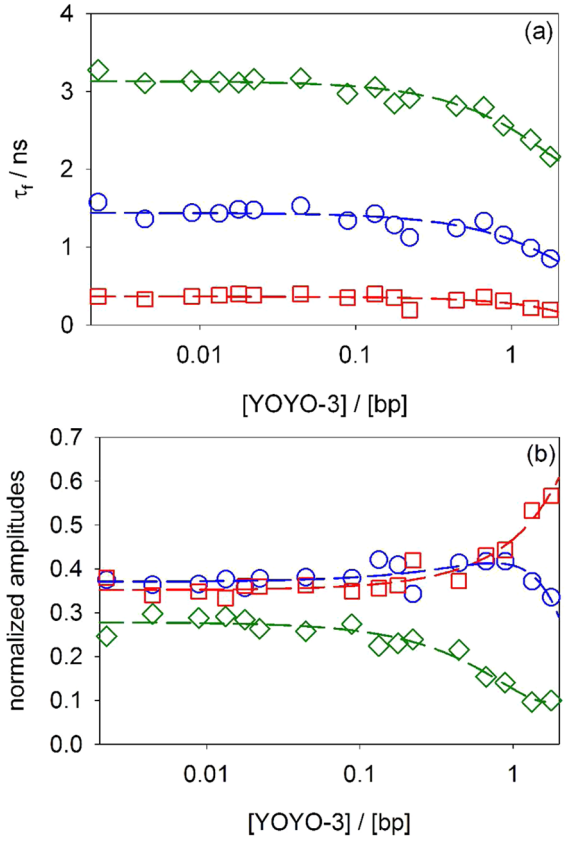

Figure 4. Semilogarithmic plots of fluorescence decay times (a) and their corresponding amplitudes (b) obtained by deconvolution analysis of the decay traces of aqueous solutions containing 0.10−0.80 μM YOYO-3 and 0.01−1.00 μM dsDNA. The symbols for the large (diamonds), intermediate (circles), and short (squares) decay times are retained for their corresponding amplitudes. The dashed lines are introduced only for illustrative purposes. λ_{ex} = 530 nm; λ_{em} = 630 nm.

Interestingly, the decay times in Figure 4a also show that the dynamic quenching of the YOYO-3 fluorescence is observed at [YOYO-3]/[DNA bp] ratios higher than 0.100. Because energy homotransfer, involving an equal nature of donor and acceptor, does not result in quenching,[56] the shortening of the YOYO-3 fluorescence decay times must be assigned to energy transfer from YOYO-3 to a different energy acceptor. Figure S-5 (Supporting Information) shows the energy transfer efficiency, Φ_{ET}, vs the [YOYO-3]/[DNA bp] ratio. Once the effective energy transfer is established, it is interesting to determine what species behaves as the energy acceptor. The species acting as an energy acceptor should be either a YOYO-3 molecule with a lower Φ_f in a different binding mode or a DNA-bound YOYO-3 aggregate. As evidenced in the single-molecule fluorescence experiments (Figure 2b) and the YOYO-3 decay times (Figure 4a), it is just at high [YOYO-3]/[DNA bp] ratios that the energy hopping is an important effect. To gain more insight into the nature of the energy acceptor, we focused on the absorption spectral changes of aqueous solutions containing

dx.doi.org/10.1021/jp303438d | J. Phys. Chem. B 2012, 116, 11561−11569

YOYO-3 and dsDNA over a large range of concentration ratios until well past the saturation conditions (Figure 5a). To

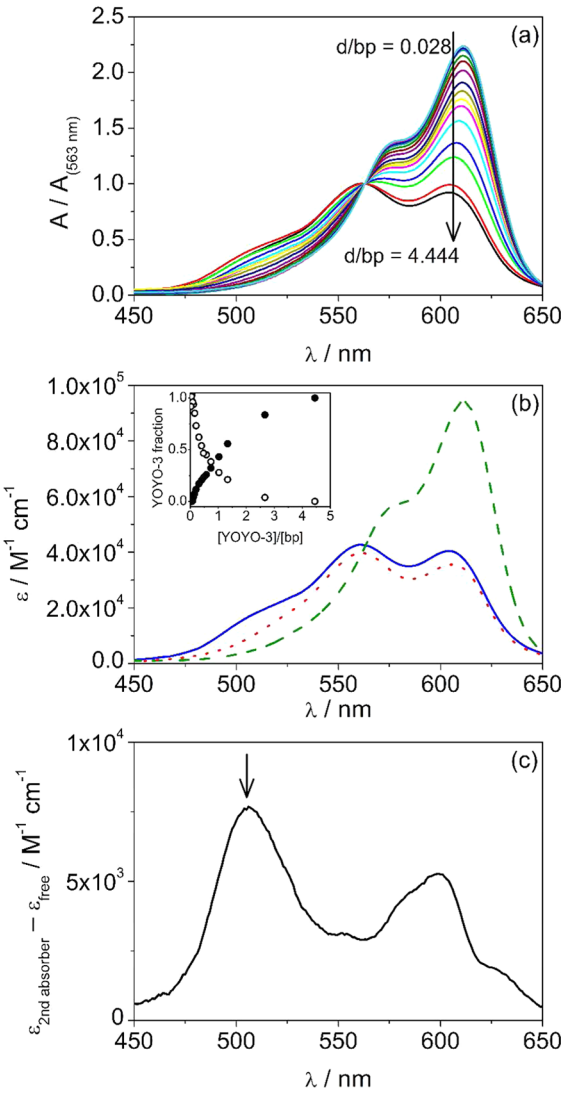

Figure 5. (a) Normalized absorption spectra of aqueous solutions containing [YOYO-3]/[DNA bp] ratios ranging from 0.028 to 4.444. (b) Molar absorption coefficients of the two YOYO-3 absorbers obtained by PCA. Dashed line: predominant absorber at low [YOYO-3]/[DNA bp] ratios. Solid line: predominant absorber at high [YOYO-3]/[DNA bp] ratios. The absorption spectrum of free YOYO-3 in aqueous solution (dotted line) is included for comparison. Inset: fractions of dsDNA-intercalated YOYO-3 (empty circles) and dsDNA-bound intramolecular YOYO-3 aggregate (filled circles). (c) Subtraction of the absorption spectrum of free YOYO-3 in aqueous solution from that of the second absorber species obtained by the PCA. Arrow indicates the presence of a blue-shifted H-aggregate.

determine the number of absorbent species responsible for the spectral variation and their corresponding molar absorption coefficients, ε, principal component analysis (PCA)[57] was employed. The results of the PCA indicate that 99.9% of the spectral variation may be assigned to only two absorbers, whose ε are shown in Figure 5b. In the inset of this figure, the fraction of YOYO-3 molecules present in each form is reported as a function of the [YOYO-3]/[DNA bp] ratio. We assign the spectral profile at low [YOYO-3]/[DNA bp] ratios to the protected, intercalated YO moieties of YOYO-3. However, at higher [YOYO-3]/[DNA bp] ratios, the shape of the spectra closely resembles that of the YOYO-3 observed in aqueous solutions devoid of DNA, clearly distinguishable by its pair of equally intense absorption bands. This second absorber at high concentrations of YOYO-3 could, in principle, be related to an excess of unbound dye that remains in solution, as the spectral profile of YOYO-3 free in solution (also shown for comparison in Figure 5b) shows two bands centered at 561 and 603 nm. Although the spectral profile of the second absorber may contain a certain contribution of free aqueous YOYO-3, several features suggest that this is not the sole influence. First, a shoulder approximately 500 nm is clearly visible in the PCA result, which is not observed in the spectrum of YOYO-3 in solution. This contribution is highlighted when the spectral profile of the free YOYO-3 in aqueous solution is subtracted from the overall spectrum of the second absorbed determined in the PCA (Figure 5c). This type of blue-shifted band is typical of parallel H-aggregates formed by dimeric cyanine dyes.[37,52,55] The plane-to-plane stacking of the two moieties results in a splitting of the excited state, with the transition to the upper state being favored and, therefore, causing a blue shift of the absorption band.[55] Second, the appearance of the second absorber is remarkable even at concentrations of YOYO-3 that are far from saturation (see inset in Figure 5b), confirming that this species is formed in the presence of DNA. Third, the magnitude of the dynamic quenching of YOYO-3 does not reach a plateau at high dye concentrations, suggesting that even at the highest studied [YOYO-3]/[DNA bp] ratios the concentration of the dsDNA-bound YOYO-3 aggregate continues to rise. It is worth noting that the efficiency of the energy transfer toward the YOYO-3 molecules that are not bound to the dsDNA is negligible at the studied concentrations. Hence, the form present at high [YOYO-3]/[DNA bp] ratios must be composed of several contributions that are indistinguishable by PCA. Interestingly, one of these contributions shows the features of an intramolecular H-aggregate, but instead of being free in solution, it appears to be bound to dsDNA. The detection of cyanine H-aggregates promoted by the presence of DNA has been previously described. For instance, we identified for a parent compound, BOBO-3, the formation of a H-aggregate specifically promoted by the presence of single-stranded DNA containing at least six consecutive cytidine nucleotides.[37] However, the H-aggregate found for YOYO-3 is facilitated in the presence of dsDNA. Therefore, it must be similar to that previously described by Armitage and colleagues, who reported the templating of H-aggregates of 3,3′-diethylthiadicarbocyanine in the minor grooves of poly(dAdT).[58] The grooves of the dsDNA structure may provide adequate pockets to promote the parallel stacking of the different moieties within the cyanine dimer, by hindering the free rotation of the linker.

To confirm that the detected YOYO-3 aggregate was indeed bound to dsDNA, we resorted to circular dichroism (CD) measurements. Importantly, by virtue of the phenomenon known as induced CD,[59] achiral molecules, like YOYO-3, show CD only when bound to chiral molecules, such as DNA. This phenomenon allows us to strictly probe bound YOYO-3 molecules, removing the contribution of YOYO-3 in solution. The recorded spectra (see Figure S-6 and Supporting Information for details) showed a CD absorption band centered at 630 nm at low [YOYO-3]/[DNA bp] ratios corresponding to the intercalated YOYO-3. However, as the ratio [YOYO-3]/[DNA bp] increases, a new duplex of bands

dx.doi.org/10.1021/jp303438d | J. Phys. Chem. B 2012, 116, 11561−11569

located near 540 nm (negative) and 585 nm (positive) become evident. This −/+ pattern, in which the integrated rotational strength is zero, is in agreement with the formation of an intramolecular aggregate[59] of the two YO moieties. Therefore, the induced CD asserts the formation of an intramolecular YOYO-3 aggregate effectively bound to dsDNA. It is worth noting that even at [YOYO-3]/[DNA bp] ratios as high as 1.334 (Figure S-6, Supporting Information) changes in the CD spectra continue to be observed. Since these changes can only arise from dsDNA bound species, this observation further confirms that the second absorber at high YOYO-3 concentrations (Figure 5b) cannot be attributed to an excess of unbound dye.

CONCLUSIONS

Herein, we have explored the changes that intercalated YOYO-3 undergoes at different dye/basepair ratios until reaching saturating conditions. The fluorescence enhancement of intercalated YOYO-3 allows it to act as an energy acceptor with a donor dye at the far end of the dsDNA molecule. Anomalies detected at the single-molecule level in the apparent FRET efficiency values and distance distributions between donor and acceptor indicated the presence of additional photophysical processes that were further investigated. First, the appearance of an intramolecular YOYO-3 aggregate with the spectral features of a H-aggregate and bound to the DNA double helix is evident in the absorption spectra (with a shoulder at 500 nm) and the circular dichroism spectra. Second, the binding of several molecules of YOYO-3 within the same dsDNA molecule facilitates intermolecular energy transfer between different units of the dye. This study provides the basis for the development of a single-molecule intercalator-based FRET strategy for signaling nucleic acid hybridization events.

ASSOCIATED CONTENT

Supporting Information

Figures S-1 to S-6 and details of the ensemble, absorption, excitation, and emission spectra, fluorescence anisotropy measurements, TRANES and SAS determination, and circular dichroism measurements. This material is available free of charge via the Internet at http://pubs.acs.org.

AUTHOR INFORMATION

Corresponding Author

*E-mail: angelort@ugr.es. Tel.: +34 958243825. Fax: +34 958244090.

Present Address

[§]School of Chemical Sciences, National Centre for Sensor Research, Dublin City University, Glasnevin, Dublin 9 (Ireland).

Author Contributions

AO, JMAP, and MJRR designed research. SGL, MJRR, and SC performed the experiments. The manuscript was written through contributions of all authors, who approve the final version of the manuscript.

Notes

The authors declare no competing financial interest.

ACKNOWLEDGMENTS

This research was supported by a Marie Curie European Reintegration Grant within the seventh European Community Framework Programme and by grant P07-FQM-3091 from the Consejería de Innovación, Ciencia y Empresa (Junta de Andalucía).

ABBREVIATIONS

FRET, Förster resonance energy transfer; SMFS, single-molecule fluorescence spectroscopy; YO, oxazole yellow; TRANES, time-resolved area-normalized emission spectra; SAS, species-associated spectra; FLDs, fluorescence lifetime distributions; BIFL, burst-integrated fluorescence lifetime

REFERENCES

(1) Borisov, S. M.; Wolfbeis, O. S. *Chem. Rev.* **2008**, *108* (2), 423−461.
(2) Berezin, M. Y.; Achilefu, S. *Chem. Rev.* **2010**, *110* (5), 2641−2684.
(3) Johansson, M. K.; Fidder, H.; Dick, D.; Cook, R. M. *J. Am. Chem. Soc.* **2002**, *124* (24), 6950−6956.
(4) Franzini, R. M.; Kool, E. T. *J. Am. Chem. Soc.* **2009**, *131* (44), 16021−16023.
(5) Newman, R. H.; Fosbrink, M. D.; Zhang, J. *Chem. Rev.* **2011**, *111* (5), 3614−3666.
(6) Cornish, P. V.; Ha, T. *ACS Chem. Biol.* **2007**, *2* (1), 53−61.
(7) Tinnefeld, P.; Sauer, M. *Angew. Chem., Int. Ed.* **2005**, *44* (18), 2642−2671.
(8) Lakowicz, J. R.; Berndt, K. W. *Rev. Sci. Instrum.* **1991**, *62* (7), 1727−1734.
(9) Laptenok, S. P.; Borst, J. W.; Mullen, K. M.; Stokkum, I. H. M. v.; Visser, A. J. W. G.; Amerongen, H. v. *Phys. Chem. Chem. Phys.* **2010**, *27*, 7593−7602.
(10) Waring, M. J. *J. Mol. Biol.* **1965**, *13* (1), 269−282.
(11) Lepecq, J. B.; Paoletti, C. *J. Mol. Biol.* **1967**, *27* (1), 87−106.
(12) Hess, S. T.; Girirajan, T. P. K.; Mason, M. D. *Biophys. J.* **2006**, *91* (11), 4258−4272.
(13) Rust, M. J.; Bates, M.; Zhuang, X. *Nat. Methods* **2006**, *3* (10), 793−796.
(14) Huang, B.; Wang, W.; Bates, M.; Zhuang, X. *Science* **2008**, *319* (5864), 810−813.
(15) Flors, C.; Ravarani, C. N. J.; Dryden, D. T. F. *ChemPhysChem* **2009**, *10* (13), 2201−2204.
(16) Talavera, E. M.; Bermejo, R.; Crovetto, L.; Orte, A.; Alvarez-Pez, J. M. *Appl. Spectrosc.* **2003**, *57*, 208−215.
(17) Wang, S.; Gaylord, B. S.; Bazan, G. C. *J. Am. Chem. Soc.* **2004**, *126* (17), 5446−5451.
(18) Xu, Q.-H.; Wang, S.; Korystov, D.; Mikhailovsky, A.; Bazan, G. C.; Moses, D.; Heeger, A. J. *Proc. Natl. Acad. Sci. U.S.A.* **2005**, *102* (3), 530−535.
(19) Talavera, E. M.; Guerrero, P.; Ocana, F.; Alvarez-Pez, J. M. *Appl. Spectrosc.* **2002**, *56*, 362−369.
(20) Rye, H. S.; Yue, S.; Wemmer, D. E.; Quesada, M. A.; Haugland, R. P.; Mathies, R. A.; Glazer, A. N. *Nucleic Acids Res.* **1992**, *20*, 2803−2812.
(21) Glazer, A. N.; Rye, H. S. *Nature* **1992**, *359*, 859−861.
(22) Haugland, R. P. *Handbook of Fluorescent Probes and Research Products*; Molecular Probes, Inc.: OR, USA, 2002.
(23) Hirons, G. T.; Fawcett, J. J.; Crissman, H. A. *Cytometry* **1994**, *15*, 129−140.
(24) Figeys, D.; Arriaga, E.; Renborg, A.; Dovichi, N. J. *J. Chromatogr. A* **1994**, *669* (1−2), 205−216.
(25) Perkins, T. T.; Quake, S. R.; Smith, D. E.; Chu, S. *Science* **1994**, *264*, 822−826.
(26) Perkins, T. T.; Smith, D. E.; Chu, S. *Science* **1994**, *264* (5160), 819−822.
(27) Larsson, A.; Carlsson, C.; Jonsson, M.; Albinsson, B. *J. Am. Chem. Soc.* **1994**, *116*, 8459−8465.
(28) Carlsson, C.; Larsson, A.; Jonsson, M.; Albinsson, B.; Norden, B. *J. Phys. Chem.* **1994**, *98* (40), 10313−10321.
(29) Leslie, A. G. W.; Arnott, S.; Chandrasekaran, R.; Ratliff, R. L. *J. Mol. Biol.* **1980**, *143*, 49−72.

(30) Arnott, S.; Chandrasekaran, R.; Hall, I. H.; Puigjaner, L. C. *Nucleic Acids Res.* **1983**, *11* (12), 4141−4155.
(31) Chuprina, V. P. *FEBS Lett.* **1985**, *186*, 98−102.
(32) Netzel, T. L.; Nafisi, K.; Zhao, M.; Lenhard, J. R.; Johnson, I. *J. Phys. Chem.* **1995**, *99* (51), 17936−17947.
(33) Rye, H. S.; Glazer, A. N. *Nucleic Acids Res.* **1995**, *23*, 1215−1222.
(34) Bowen, B. P.; Enderlein, J.; Woodbury, N. W. *Photochem. Photobiol.* **2003**, *78* (6), 576−581.
(35) Ruedas-Rama, M. J.; Orte, A.; Crovetto, L.; Talavera, E. M.; Alvarez-Pez, J. M. *J. Phys. Chem. B* **2010**, *114*, 1094−1103.
(36) Ruedas-Rama, M. J.; Alvarez-Pez, J. M.; Paredes, J. M.; Talavera, E. M.; Orte, A. *J. Phys. Chem. B* **2010**, *114*, 6713−6721.
(37) Ruedas-Rama, M. J.; Alvarez-Pez, J. M.; Orte, A. *J. Phys. Chem. B* **2010**, *114*, 9063−9071.
(38) Lakowicz, J. R. *Principles of Fluorescence Spectroscopy*, 3rd ed.; Springer: New York, 2006.
(39) Wahl, M.; Erdmann, R.; Lauritsen, K.; Rahn, H. J. *Proc. SPIE* **1998**, *3259*, 173−178.
(40) Benda, A.; Hof, M.; Wahl, M.; Patting, M.; Erdmann, R.; Kapusta, P. *Rev. Sci. Instrum.* **2005**, *76*, 033106.
(41) Eggeling, C.; Berger, S.; Brand, L.; Fries, J. R.; Schaffer, J.; Volkmer, A.; Seidel, C. A. *J. Biotechnol.* **2001**, *86* (3), 163−80.
(42) Barber, P. R.; Ameer-Beg, S. M.; Pathmananthan, S.; Rowley, M.; Coolen, A. C. C. *Biomed. Opt. Express.* **2010**, *1*, 1148−1158.
(43) Orte, A.; Clarke, R. W.; Klenerman, D. *Anal. Chem.* **2008**, *80* (22), 8389−8397.
(44) Gell, C.; Brockwell, D.; Smith, A. *Handbook of single molecule fluroescence*; Oxford University Press: Oxford (U.K.), 2006.
(45) Neuweiler, H.; Sauer, M. *Anal. Chem.* **2005**, *77* (9), 178 A−185 A.
(46) Pappas, D.; Burrows, S. M.; Reif, R. D. *TrAC, Trends Anal. Chem.* **2007**, *26* (9), 884−894.
(47) Orte, A.; Clarke, R.; Klenerman, D. *Biochem. Soc. Trans.* **2010**, *038* (4), 914−918.
(48) Bustamante, C.; Bryant, Z.; Smith, S. B. *Nature* **2003**, *421*, 423−427.
(49) Benvin, A. L.; Creeger, Y.; Fisher, G. W.; Ballou, B.; Waggoner, A. S.; Armitage, B. A. *J. Am. Chem. Soc.* **2007**, *129* (7), 2025−2034.
(50) Cosa, G.; Focsaneanu, K. S.; McLean, J. R. N.; McNamee, J. P.; Scaiano, J. C. *Photochem. Photobiol.* **2001**, *73* (6), 585−599.
(51) Fürstenberg, A.; Julliard, M. D.; Deligeorgiev, T. G.; Gadjev, N. I.; Vasilev, A. A.; Vauthey, E. *J. Am. Chem. Soc.* **2006**, *128* (23), 7661−7669.
(52) Fürstenberg, A.; Vauthey, E. *J. Phys. Chem. B* **2007**, *111* (43), 12610−12620.
(53) Hannestad, J. K.; Sandin, P.; Albinsson, B. *J. Am. Chem. Soc.* **2008**, *130*, 15889−15895.
(54) Dale, R. E.; Einsinger, J.; Blumberg, W. E. *Biophys. J.* **1979**, *26*, 161−194.
(55) Fürstenberg, A.; Deligeorgiev, T. G.; Gadjev, N. I.; Vasilev, A. A.; Vauthey, E. *Chem.−Eur. J.* **2007**, *13* (30), 8600−8609.
(56) Nemkovich, N. A.; Rubinov, A. N.; Tomin, V. I. In *Topics in Fluorescence Spectroscopy*; Lakowicz, J. R., Ed.; Kluwer Academic Publishers: New York, 2002; Vol. 2, Principles, p 390.
(57) Malinowski, E. R. In *Factor Analysis in Chemistry*, 3rd ed.; John Wiley and Sons: New York, 2002.
(58) Seifert, J. L.; Connor, R. E.; Kushon, S. A.; Wang, M.; Armitage, B. A. *J. Am. Chem. Soc.* **1999**, *121* (13), 2987−2995.
(59) Cantor, C. R.; Schimmel, P. R. In *Biophysical Chemistry, Part II: Techniques for the study of biological structure and function*; W. H. Freeman & Company: San Francisco, CA, 1980; pp 392−463.